Electric Vehicle Charge Cycle Management System for ComEd Real-Time Pricing Scheme: An IoT Solution

Miguel Ángel Dávila Rojas and César Leonardo Trujillo Rodríguez

***Abstract*—In this article, an electric vehicle (EV) charge cycle management system (CCMS) for ComEd real-time pricing (RTP) scheme is presented. It is an embedded system for an EV smart charger. As an energy management system, implemented system seeks to reduce charge cycle cost per kWh. Charge cycle management is performed in three steps: first, prices are forecasted along the available time horizon through a trend and seasonality model. Thereafter, with the aim of scheduling the charge cycle, the lowest pricing intervals combination is found using a direct insertion sort algorithm. Finally, the scheduled combination is executed with possible adjustments on execution time in function of the current price. Algorithm performance is evaluated on a simulation study where user daily routine and user driving behavior are modeled stochastically and ComEd RTP historical data are used.**

***Index Terms*—Demand-side management (DSM), electric vehicle (EV) charging, energy management systems, Internet of Things (IoT), real-time systems, scheduling algorithms, smart devices.**

I. Introduction

THE BALANCE between generated and consumed power in a distribution grid operation is a critical issue for grid reliability. However, the demand is variable in time with high unexpected peaks or drastic drops. The available electric power can also be variable in time depending on the availability of the resource from which it is generated. Moreover, power sources have different operational flexibilities, which makes it difficult to manage power generation to achieve such balance. Additionally, the increasingly widespread use of electric vehicles (EVs) has a huge impact due to the amount of electrical energy needed to perform charging processes, uncoordinated charges can result in huge unwanted demand spikes [1].

Demand-side management (DSM) is another viable strategy that consists in making use of operational flexibilities provided by some loads such as EVs. The demand can be regulated by giving economic incentives to consumers to decrease or increase their consumption when grid operation requires it. Depending on the approach, DSM strategies can be classified into direct load control (DLC) and variable pricing schemes. DLC programs are based on contracts in which customers permit utility operators to turn off some loads during emergencies or high demand peaks in exchange for compensation [2]–[8]. However, when there is a large customer base, DLC programs require a centralized control scheme with complex communication and computation requirements [9]. In contrast, variable pricing schemes do not require such infrastructure deployment because customers regulate their consumption in response to the price set at the wholesale interchange market [10]–[13].

In spot energy markets, the prices are set in real time and known to the public almost as soon as deals are transacted. In an RTP scenario, the demand response could hardly be in real time because it depends on the customer's consumption management. To take advantage of the operational flexibilities provided by some loads such as EVs, it is required to implement smart devices and mechanisms, with low communication and computation requirements, to automatically manage the consumption in response to the RTP signal. This is the necessity that this project pretends to tackle. Addressing this issue, in this article, we present the design of an IoT-based charge cycle management system (CCMS) that could be incorporated into an EV smart battery charger to automatically manage the EV charge cycle consumption in response to an RTP signal. In the next paragraph, related IoT-based approaches, to tackle the above-mentioned issue, are summarized.

The Internet of Things (IoT) concept has been applied in the smart grid (SG) context where the interconnection between everyday objects through the Internet could be a suitable solution in order that energy consumption could be managed without human intervention [14]–[23]. A distributed online algorithm for optimal real-time energy distribution was proposed in [14], where each user deploys a smart meter so that power grid operator can monitor and control the energy consumption of their electrical appliances. In [15], energy management and demand reduction are based on energy demand forecasting for each consumer through time-series analysis. Consumer historical data is collected in an IoT-Fog network based on smart meters and fog routers. In [16], Social Internet of Energy (SIoE) is proposed as a DSM strategy in the SG context, grouping prosumers by their energy load shape compatibility and then rescheduling intragroup load shapes. In [17], a narrowband-IoT (NB-IoT) system to monitor and control electrical appliances in an SG is presented. NB-IoT

Manuscript received 14 December 2021; revised 23 April 2022; accepted 1 July 2022. Date of publication 13 July 2022; date of current version 25 April 2023. *(Corresponding author: Miguel Ángel Dávila Rojas.)*

Miguel Ángel Dávila Rojas is with the Alternative Energy Sources Research Laboratory LIFAE, Universidad Distrital Francisco José de Caldas, Bogotá 110231, Colombia (e-mail: miadavilar@correo.udistrital.edu.co).

César Leonardo Trujillo Rodríguez is with the Department of Electrical Engineering, Universidad Distrital Francisco José de Caldas, Bogotá 110231, Colombia (e-mail: cltrujillo@udistrital.edu.co).

Digital Object Identifier 10.1109/JIOT.2022.3190453

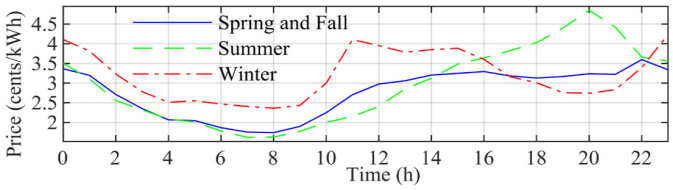

Fig. 1. Average daily pattern of ComEd electricity price.

is an IoT cellular solution, and the proposed architecture is composed of customer monitoring units, a database server, and a demand response controller in which the DSM strategy is centralized.

The main contribution of this article is to propose CCMS as a DSM IoT solution for an EV smart charger that autonomously and automatically manages the charge cycle in real time as a response to ComEd RTP signal. With a simpler network architecture than the above-mentioned approaches, our approach only requires a residential AP to access the Internet. In addition, the proposed CCMS does not require that EV users share their consumption behavior data to manage their consumption.

The outline of this article is as follows: a ComEd RTP signal analysis is presented in Section II, ComEd RTP signal modeling is presented in Section III, the proposed CCMS architecture is presented in Section IV, the proposed charge cycle management algorithm (CCMA) is presented in Section V, an evaluation of the algorithm performance through a simulation study is presented in Section VI, experimental validation of the proposed system is shown in Section VII, and the conclusion and future work are presented in Section VIII.

II. ComEd Real-Time Pricing Signal Analysis

In an RTP scheme, price is set in real time at wholesale markets to meet a balance between available energy supply and energy demand. Despite final users do not take part in the wholesale market, their demand is aggregated by retailers who provide them electricity. Since electricity price is defined only for the current pricing interval, electricity price needs to be forecasted to schedule future electricity consumption along the available time horizon to perform the EV charge cycle. In this article, it is considered the scenario where ComEd is the utility company that provides electricity to EV user at PJM wholesale market price. Thus, the ComEd RTP price signal must be forecasted, for that purpose, analysis, and modeling of the ComEd price signal are exposed next.

As it is shown in Fig. 1, the price signal has a daily pattern with the highest rates at peak demand time intervals and the lowest rates at the lowest demand time intervals. Its highest variations depend on the season of the year with lower variations due to the day of the week. Fig. 1 shows the daily pattern by season based on the hourly average of electricity prices. The pattern is obtained from ComEd price historical data, available through ComEd API [24], by averaging the prices filtered by the season of the year and hour of the day.

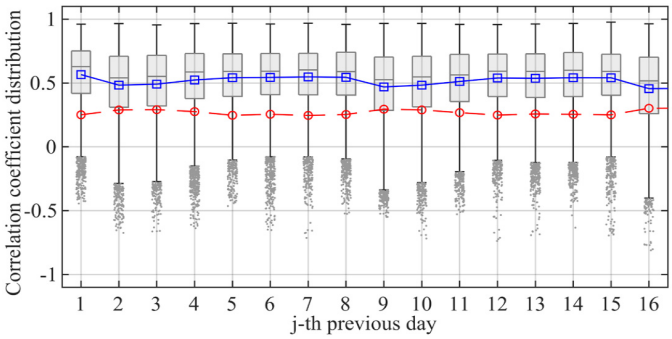

Fig. 2. Distributions of correlations coefficients with the jth previous day ($j = 1, \ldots, 16$) when current day is Monday; mean in a solid line with square markers and standard deviation in a dashed line with circle markers.

TABLE I
Previous Day Most Correlated With Each Day of the Week

Day	j	$\mu_{r_{xx_j}}$	$\sigma_{r_{xx_j}}$	*Description*
Monday	1	0.566	0.251	Previous day
Tuesday	7	0.573	0.244	Same day previous week
Wednesday	7	0.534	0.285	Same day previous week
Thursday	1	0.492	0.319	Previous day
Friday	1	0.531	0.287	Previous day
Saturday	1	0.564	0.256	Previous day
Sunday	1	0.575	0.257	Previous day

To find which prices from the past should be used to forecast price signal along the available time horizon, population Pearson's correlation coefficient between current daily patterns and previous days patterns are estimated through sample correlation. Given a column vector $P = [p_n]$, for $1 \leq n \leq L$ ($L = 903825$), whose components are ComEd historical price data [24] every pricing interval ($T_s = 5$ min) from 2012-10-29 04:20:00 to 2021-06-02 11:00:00. $x = [p_{n+k}]$ for $k = 0, 1, \ldots, N$, are prices of some day starting at n; $x_j = [p_{(n-jN)-k}]$ for $k = 0, 1, \ldots, N$ and $j = 1, 2, \ldots, D$, are prices of the jth previous day; where $N = 288$ is the number of pricing intervals in one day and D is the number of previous considered days. Then, sample correlation between samples x and x_j is calculated as

$$r_{xx_j} \stackrel{\text{def}}{=} \frac{\sum_{k=1}^{N} (x_k - \bar{x})(x_{j,k} - \bar{x_j})}{(N-1)s_x s_{x_j}} = \frac{\sum_{k=1}^{N} (x_k - \bar{x})(x_{j,k} - \bar{x_j})}{\sqrt{\sum_{k=1}^{N} (x_k - \bar{x})^2 \sum_{k=1}^{N} (x_{j,k} - \bar{x_j})^2}} \quad (1)$$

where s_x and s_{x_j} are, respectively, sample standard deviations of x and x_j, and the bar operator denotes sample mean.

Once each correlation coefficient distribution was estimated, the previous days most correlated with each day of the week were found. Fig. 2 shows the correlation coefficient distribution with the jth previous day ($j = 1, \ldots, 16$) when current day is Monday. Table I presents mean $\mu_{r_{xx_j}}$ and standard deviation $s_{r_{xx_j}}$ of distribution of such correlation coefficients for each day of the week.

III. ComEd Real-Time Pricing Signal Modeling

From ComEd historical price data $P = [p_n]$, the price signal could be represented as a discrete-time signal $y = \{y[k]\}$ with sample period $T_s = 5$ min, whose kth price value is $y[k] =$

p_{n+k-jN} for $-N \le k \le T_{\text{in}}$ and j is defined as (2) according to Table I, where $N = 288$ is the number of sample periods T_s on one day, p_n is the price at user arrival time to home T_{arr}, and $T_{\text{in}} = (T_{\text{dep}} - T_{\text{arr}})/T_s$ is the number of sample periods T_s available to perform charge cycle until user departure time from home T_{dep}

$$j = \begin{cases} 0 \text{ if } T_{\text{arr}} \in \{\text{Mon., Thu., Fri., Sat., Sun.}\} \\ 6 \text{ if } T_{\text{arr}} \in \{\text{Tue., Wed.}\}. \end{cases} \tag{2}$$

To forecast $y = \{y[k]\}$ at arrival time T_{arr} along available time horizon $0 \le k \le T_{\text{in}}$, price signal $y = \{y[k]\}$ must be modeled. In the time-series analysis approach, $y[k]$ needs to be decomposed as a combination of trend, seasonality, and residual error. Here, decomposition of additive form is considered, price signal is modeled as $y = \{y[k]\} = \{t[k] + s[k] + w[k]\}$ where $t = \{t[k]\}$ is a trend line, $s = \{s[k]\}$ is the seasonal component or price signal periodicity, and $w = \{w[k]\}$ is the residual error which is a random sequence with mean $\mu_w = 0$ and some variance s_w^2. The trend line could be found easily through linear regression, seasonality models could also be adjusted at a low computational cost, but the residual error should be modeled through statistical models, machine learning, or hybrid models all of them at a high computational cost. Because it is desirable that the price signal model must have low computational cost, price signal is approximated as $y \sim \{\widehat{y}[k]\} = \{t[k] + s[k]\}$, adjusted for previous day prices values $-N \le k \le 0$ and projected for $0 \le k \le T_{\text{in}}$ to forecast price signal along available time horizon.

A. Trend Models

Two models for trend line are considered, a linear regression $t[k] = \beta_0 + \beta_1 k$ adjusted through: ordinary least squares (OLS) and weighted least squares (WLS), the former on homoscedasticity assumption and the latter on heteroscedasticity assumption.

1) Linear Regression With Ordinary Least Squares: The OLS problem f is formulated as (3), where β_0 and β_1 are real numbers which minimize the sum of squares of residual errors $e[k] = y[k] - t[k]$ for $-N \le k \le 0$. Solving the couple of linear equations $\partial\varphi/\partial\beta_0 = 0$ y $\partial\varphi/\partial\beta_1 = 0$ for $\beta_0, \beta_1, \varphi$ problem can be analytically solved as it is shown in (4) and (5)

$$\varphi = \min_{\beta_0,\beta_1 \in R} \sum_{k=-N}^{0} (e[k])^2 = \min_{\beta_0,\beta_1 \in R} \sum_{k=-N}^{0} (y[k] - (\beta_0 + \beta_1 k))^2 \tag{3}$$

$$\beta_1 = \frac{12}{N^3 + 3N^2 + 2N} \sum_{k=-N}^{0} \left(\left(k + \frac{N}{2} \right) y[k] \right)$$

$$\beta_1 = \frac{\sum_{k=-288}^{0} ((k + 144) y[k])}{2011440}. \tag{4}$$

$$\beta_0 = \frac{N}{2}\beta_1 + \frac{1}{N+1} \sum_{k=-N}^{0} y[k],\ \beta_0 = 144\beta_1 + \frac{\sum_{k=-288}^{0} y[k]}{289}. \tag{5}$$

2) Linear Regression With Weighted Least Squares: Due to outlier price signal values, trend line adjusted with OLS is a biased estimator of real trend. To find a better approximation to the best linear unbiased estimator (BLUE), the WLS approach is considered. The WLS problem φ is formulated as (6), where β_0 and β_1 are real numbers which minimize the weighted sum of squares of residual errors $e[k] = y[k] - t[k]$ for $-N \le k \le 0$. Once again, solving the couple of linear equations $\partial\varphi/\partial\beta_0 = 0$ y $\partial\varphi/\partial\beta_1 = 0$ for $\beta_0, \beta_1, \varphi$ problem can be analytically solved as it is shown in (7) and (8)

$$\varphi = \min_{\beta_0,\beta_1 \in R} \sum_{k=-N}^{0} \omega_k (y[k] - (\beta_0 + \beta_1 k))^2. \tag{6}$$

$$\beta_1 = \frac{\sum_{k=-N}^{0} k\omega_k y[k] \sum_{k=-N}^{0} \omega_k - \sum_{k=-N}^{0} \omega_k y[k] \sum_{k=-N}^{0} k\omega_k}{\sum_{k=-N}^{0} \omega_k \sum_{k=-N}^{0} k^2\omega_k + \frac{N(N+1)}{2} \sum_{k=-N}^{0} k\omega_k}. \tag{7}$$

$$\beta_0 = \frac{\sum_{k=-N}^{0} \omega_k y[k] + \frac{N(N+1)}{2}\beta_1}{\sum_{k=-N}^{0} \omega_k}. \tag{8}$$

WLS is a particular case of generalized least squares (GLS), WLS arises when the variances of the observed values are unequal, and no correlations exist among the observed variances (heteroscedasticity). Consequently, parameters β_0 and β_1 determine the BLUE when $\omega_k = 1/s_k^2$, where $s_{y[k]}^2$ is the variance of the kth price value $y[k]$ then the better the estimation of $s_{y[k]}^2$, the better the approximation to the BLUE. $s_{y[k]}^2$ is estimated for $k = -N, \ldots, 0$ through sample variance $s_{y[k]}^2$ of a subset with length $a = a_2 - a_1$ in the neighborhood of $y[k]$, as it is shown in (9). Parameter $a = 15$ centered at k ($a = \{2a + 1 | a \in N^+\}$) is selected such that statistically minimize MAE (10) when modeling trend for several experiments with ComEd historical price data $P = [p_n]$, then $a_1 = -(a-1)/2$ and $a_2 = (a-1)/2$

$$\begin{aligned} s_k^2 &= \frac{1}{a} \sum_{i=a_1}^{a_2} \left(y[k-i] - \bar{y}_{k,a} \right)^2 \\ &= \frac{1}{a} \sum_{i=a_1}^{a_2} \left(y[k-i] - \frac{1}{a} \sum_{j=a_1}^{a_2} y[k-j] \right)^2. \end{aligned} \tag{9}$$

$$\text{MAE} = \frac{1}{N} \sum_{k=-N}^{0} |e[k]| = \frac{1}{N} \sum_{k=-N}^{0} |y[k] - t[k]|. \tag{10}$$

B. Seasonality Models

Two common models for seasonality are considered to get the sequence $s = \{s[k]\}$ from detrended the price signal $q[k] = y[k] - t[k]$ for $-N \le k \le 0$, sequence that would be the same for next period $0 \le k \le N$ which contains available time horizon $0 \le k \le T_{\text{in}}$, considered models are as follows.

1) Simple Moving Average Filter: The kth value of sequence $s = \{s[k]\}$ is obtained smoothing the detrended sequence $q = \{q[k]\}$ through a simple moving average (SMA) filter for $-N \le k \le 0$, as it is shown in

$$s[k] = \frac{1}{M+1} \sum_{i=0}^{M} q[k-i] \tag{11}$$

where M is the moving window length, its value and position around $q[k]$ are adjusted to maximize the mean absolute scaled error (MASE) (16).

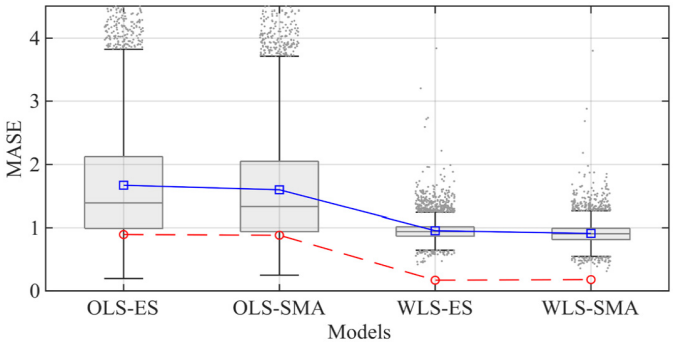

Fig. 3. Distributions of MASE: mean in a solid line with square markers and standard deviation in a dashed line with circle markers.

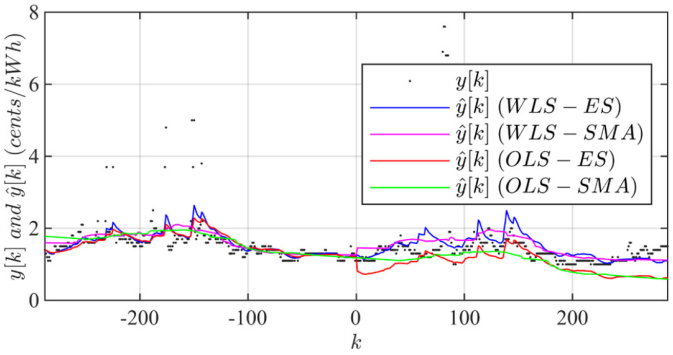

Fig. 4. Price $y[k]$ and forecasted price $\widehat{y}[k]$ for $-N = k = N$ with T_{arr} $(k = 0)$ at Sunday 5 April 2020 at 12:20.

2) First-Order Exponential Smoothing: The kth value of sequence $s = \{s[k]\}$ is obtained smoothing the detrended sequence $q = \{q[k]\}$ by introducing geometrically decreasing weightings to the sum of past values of the sequence and then normalizing it by the sum of those weightings

$$s[k] = \frac{\sum_{i=0}^{k+N} \theta^i q[k-i]}{\sum_{i=0}^{k+N} \theta^i} = \frac{1-\theta}{1-\theta^{k+N+1}} \sum_{i=0}^{k+N} \theta^i q[k-i]$$
$$\cong (1-\theta) \sum_{i=0}^{k+N} \theta^i q[k-i]. \tag{12}$$

According to the following procedure:

$$s[k] = (1-\theta)q[k] + (1-\theta)\Big(\theta q[k-1] + \theta^2 q[k-2] + \cdots + \theta^{k+N} q[-N]\Big). \tag{13}$$

$$s[k] = (1-\theta)q[k] + \theta(1-\theta)\Big(q[k-1] + \theta q[k-2] + \cdots + \theta^{k-1+N} q[-N]\Big). \tag{14}$$

$$s[k] = (1-\theta)q[k] + \theta s[k-1]. \tag{15}$$

The kth value of sequence $s = \{s[k]\}$ can be calculated recursively as $s[k] = \lambda q[k] + (1-\lambda)s[k-1]$, for $-N \leq k \leq 0$ and $0 < \lambda < 1$ where discount factor $\lambda = 1 - \theta$ is the parameter to be adjusted to maximize the MASE (16) and can be assumed that $s_o = s[-N-1] = q[-N]$ for the first iteration.

C. Fitting and Validating Models

Seasonal Naïve is the simplest and lowest computational cost model due to the assumption that sequence $y = \{y[k]\}$ is periodic and can be approximated by $\widehat{y}[k] = y[k-N-1]$ for $k = 1, \ldots, N$. The MASE is the MAE (10) due to model forecasting scaled by MAE due to Seasonal Naïve forecasting, it is expressed mathematically as

$$\text{MASE} = \frac{1}{N} \sum_{k=1}^{N} \frac{|e_k|}{\frac{1}{N}\sum_{k=1}^{N} |\widehat{e}_k|} = \frac{\sum_{k=1}^{N} |y[k] - \widehat{y}[k]|}{\sum_{k=1}^{N} |y[k] - y[k-N-1]|}. \tag{16}$$

The parameters of the models were fitted for historical price data $P = [p_n]$ through a fourfold cross validation to get the minimum MASE, MASE statistics are shown in Fig. 3. An example of price forecasting for 5 April 2020 at 12:20 is shown in Fig. 4.

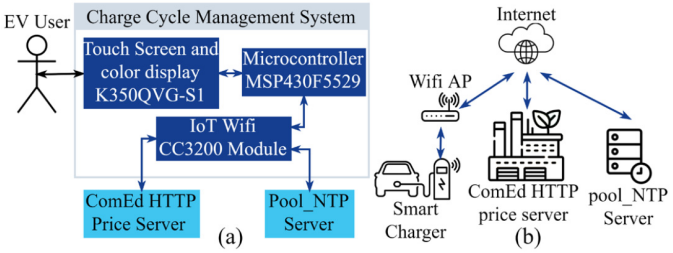

Fig. 5. (a) System hardware architecture and (b) network architecture.

IV. Charge Cycle Management System Architecture

To manage the charge cycle in real time and automatically, the CCMS is proposed as an application of the IoT concept. Consequently, it is proposed as an embedded system for a smart charger, it can access the Internet through a Texas Instruments (TI) CC3200 Wi-Fi and IoT module. The proposed CCMA, which is presented below, is embedded in a TI MSP430F5529 microcontroller. Interaction with EV user is done through a K350QVG touch screen and color display, which is controlled by MSP430F5529, in which a Graphical User Interface was implemented. The system hardware architecture is represented in the block diagram in Fig. 5(a). Communication between the K350QVG display and MSP430F5529 is implemented through an SPI peripheral and analog-to-digital conversion (ADC) for a resistive touch screen. Communication between MSP430F5529 and CC3200 module is implemented through a UART peripheral. Communication between the CCMS and servers is performed through the Internet, as it is shown in network architecture in Fig. 5(b).

The CC3200 module is configured as a Wi-Fi Station (STA) to access the Internet when it is connected to a Wi-Fi access point (AP) at the user residential LAN. Then, prices are queried to theComEd price server through the HTTP protocol according to ComEd 5-Min Price Data API [24]. To synchronize the charge cycle process, time is obtained from an NTP server through the NTP protocol. Fig. 6 shows CCMS interactions with EV user, system hardware components, HTTP, and NTP servers while charge cycle management is performing.

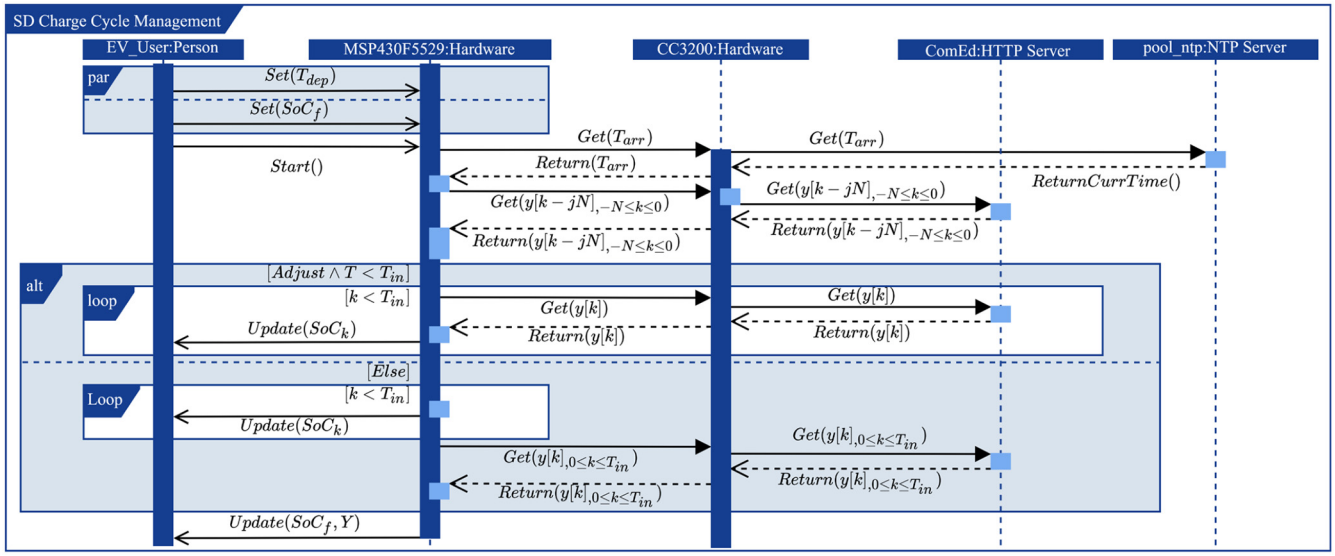

Fig. 6. Charge cycle management process sequence diagram.

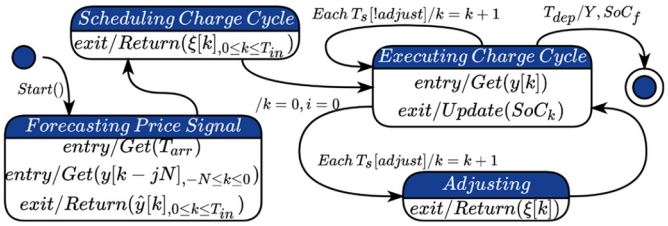

Fig. 7. State diagram representation for CCMA.

V. Charge Cycle Management Algorithm

The state diagram in Fig. 7 shows CCMS behavior when it performs the following three tasks: 1) price signal forecasting; 2) pricing intervals combination schedule; and 3) charge cycle execution. It is composed of four states, starting at price signal forecasting when the EV user starts the process, then a transition to charge cycle scheduling state occurs. On scheduling completion, the system transits to charge cycle execution where the charge cycle is performed according to pricing intervals scheduled combination. On real-time execution, the scheduled combination can be adjusted depending on EV user preference. Algorithms for each task are exposed as follows.

A. Price Signal Forecasting Algorithm

It consists of forecasting price signal along the available time horizon to perform the charge cycle. To illustrate this procedure, the correspondent flowchart is shown in Fig. 8(a) and interactions between actors and system components are presented in the sequence diagram of Fig. 6. As it is shown in Fig. 8(a), given departure time T_{dep} introduced by EV user and arrival time obtained from an NTP server, the system computes the number of available pricing intervals T_{in}. After that, previous day prices $y[k - jN]$ for $-N \leq k \leq 0$ are obtained from the ComEd server according to Table I. Finally, forecasted price signal $\widehat{y}[k]$ for $0 = k < T_{\text{in}}$ is calculated from the previous day price signal $y[k - jN]$ according to the ComEd RTP signal models presented above.

B. Charge Cycle Scheduling Algorithm

The flowchart for the charge cycle scheduling algorithm is shown in Fig 8(c). First, to reach the SoC_f introduced by the EV user, the number of needed pricing intervals to perform the charge cycle is calculated. Then, given the number of available pricing intervals T_{in}, the combination of needed pricing intervals T_N, which results in the lowest cost per kWh defined as (17), is found

$$Y = \left(\sum_{k=0}^{(T_{\text{in}}-1)} \xi[k] y[k] \right) / \left(\sum_{k=0}^{(T_{\text{in}}-1)} \xi[k] \right) \tag{17}$$

where $\xi[k]$ for $0 \leq k < T_{\text{in}}$ is a sequence of numbers with $\xi[k] = 1$ if the kth pricing interval belongs to the lowest cost per kWh combination, else $\xi[k] = 0$. If the number of needed pricing intervals T_N is greater or equal to the number of available pricing intervals T_{in}, scheduled combination $\xi[k] = 1$ for $0 \leq k < T_{\text{in}}$ (the whole available time to perform charge cycle). Otherwise, scheduled combination $\xi[k]$ for $0 \leq k < T_{\text{in}}$ is found through direct insertion sort algorithm whose flowchart representation is presented in Fig. 8(b) (see [26] for an explanation about direct insertion sort). Forecasted price signal and its time index are stored in an array $Z_{k,i} = [\widehat{y}[k]\ k]_{,0=k<T_{\text{in}};i=1,2}$, $Z_{k,i}$ is sorted by first column $Z_{k,1}$, then sorted $Z_{k,1} = 1$ for $0 \leq k \leq T_N$ and sorted $Z_{k,1} = 0$ for $T_N < k < T_{\text{in}}$. After that, resulting array is sorted by its second column $Z_{k,2}$ to get scheduled combination as $\xi[k] = Z_{k,1}$ for $0 \leq k < T_{\text{in}}$.

C. Charge Cycle Real-Time Execution Algorithm

Once a pricing intervals combination has been scheduled to perform charge cycle, the system falls into executing charge cycle state where it stays most of the time. In this state, the

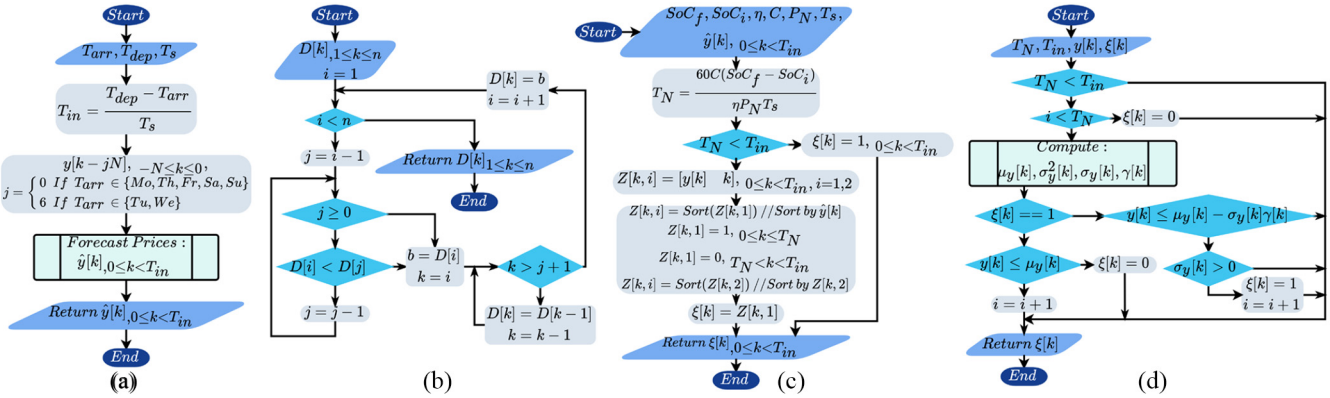

Fig. 8. Flowcharts: (a) price signal forecasting algorithm, (b) direct insertion sort algorithm, (c) scheduling algorithm, and (d) real-time adjusting algorithm.

charge cycle is executed in real time (each pricing interval T_s) according to scheduled pricing intervals combination.

As it is shown in the sequence diagram in Fig. 6 and the state diagram in Fig. 7, cumulative SoC_k, defined as (18), is updated for each pricing interval T_s ($0 \le k < T_{\mathrm{in}}$).

$$\mathrm{SoC}_k = \mathrm{SoC}_{k-1} + \left(\eta P_N T_S/60C\right)\xi[k]. \tag{18}$$

As it is also shown in Figs. 6 and 7, at T_{dep} when available time to perform charge cycle ends ($k = T_{\mathrm{in}}$), cost per kWh is calculated as (17) and SoC_f as

$$\mathrm{SoC}_f = \mathrm{SoC}_i + \left(\eta P_N T_S/60C\right) \sum_{k=0}^{(T_{\mathrm{in}}-1)} \xi_e[k] \tag{19}$$

where $\xi_e[k]$ for $0 \le k < T_{\mathrm{in}}$ is the pricing intervals combination in which charge cycle was executed.

On execution state, transitions to adjusting state can occur for each pricing interval T_s if adjust option is chosen. So that unexpected outlier prices within RTP signal due to errors on forecasting $y[k]$ for $0 \le k < T_{\mathrm{in}}$ can be considered on execution time. It is desirable that lower outlier pricing intervals, which were not initially considered on scheduling, can be used to perform charge cycle and higher outlier pricing intervals, which were initially considered on schedule, can be avoided. Thus, outlier prices must be identified and $\xi[k]$ for $0 \le k < T_{\mathrm{in}}$ must be modified on execution time. In such a case, scheduled combination $\xi[k]$ is modified for each pricing interval ($0 \le k < T_{\mathrm{in}}$) according to the real-time adjusting algorithm illustrated in the flowchart in Fig. 8(d). For each price interval in $0 \le k < T_{\mathrm{in}}$, the charge process is performed according to scheduled combination $\xi[k]$, but if current price is a low outlier price and it was not originally scheduled it will be included in such combination ($\xi[k] = 1$). On the other hand, if the current price is a high outlier price, it will be excluded from such combination ($\xi[k] = 0$) even if it was originally considered in it.

To identify outlier prices, price signal mean μ_y and variance s_y^2 are estimated for each instant k, respectively, as (20) and (21). Standard deviation can be estimated through the variance as $s_y[k] = (s_y^2[k])^{1/2}$ for $0 \le k < T_{\mathrm{in}}$. Higher outlier pricing intervals are those whose prices are some standard deviations greater than the mean price. Similarly, lower outlier pricing intervals are those whose prices are some standard

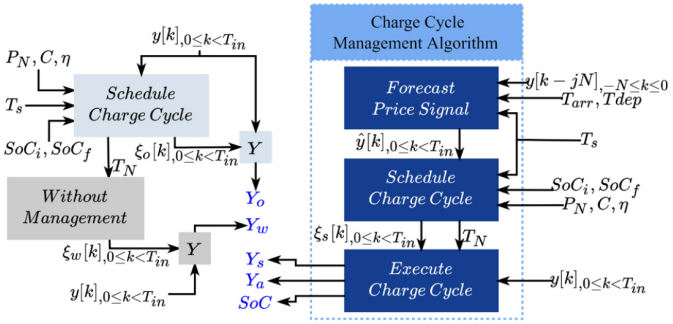

Fig. 9. Simulation scenario diagram.

deviations below the mean price. A γ function is introduced to weigh how many standard deviations above or below the mean price should be considered to identify outlier prices. For simplicity and due to the fact that μ_y and s_y estimations are worse at the beginning of charge cycle, γ function is chosen as $\gamma[k] = a - (\beta/T_{\mathrm{in}})k$ for $0 \le k < T_{\mathrm{in}}$, a decreasing linear function of k to make the criteria more flexible when k tends to T_{in}. The values $a = 4.5$ and $\beta = 4.5$ are statistically adjusted for ComEd historical price data $P = [p_n]$ to maximize percentage saving (22) and minimize SoC error (23) obtained with executed pricing intervals combination $\xi_e[k]_{,0\le k<T_{\mathrm{in}}}$

$$\mu_y[k] = \begin{cases} y[k], & \text{if } k = 0 \\ \left((k-1)\mu_y[k-1] + y[k]\right)/k, & \text{if } 0 < k < T_{\mathrm{in}}. \end{cases} \tag{20}$$

$$s_y^2[k] = \begin{cases} 0, & \text{if } k = \{0, 1\} \\ \left((k-2)s_y^2[k-1] + (y[k] - \mu_y[k])^2\right)/(k-1), & \text{if } 1 < k < T_{\mathrm{in}}. \end{cases} \tag{21}$$

VI. Simulation Study

A simulation study is done to evaluate the proposed CCMA performance under usual conditions. First, the simulation scenario is presented, then implemented models for stochastic variables are exposed and finally simulation results are shown and discussed.

A. Simulation Scenario

The implemented simulation scenario is illustrated in diagram in Fig. 9. There are four cases considered where

3100 simulation experiments are accomplished assuming constant power charging method, all of them with fixed input variables, such as $P_N = 10$ kW, $\eta = 0.85$, $C = 80$ kWh, $T_s = 5$ min, and $\text{SoC}_f = 100\%$, random input variables, such as SoC_i T_{arr}, T_{dep}, and the ComEd historical price data $P = [p_n]$ for $y[k]$ $0 \leq k < T_{\text{in}}$. Following four cases are considered for each simulation experiment.

1) Optimal Pricing Intervals Combination: Actual price signal $y[k]$ for $0 \leq k < T_{\text{in}}$ is known at scheduling time. Optimal combination $\xi_o[k]$ for $0 \leq k < T_{\text{in}}$ is obtained through the scheduling algorithm with actual price signal $y[k]$ for $0 \leq k < T_{\text{in}}$, then optimal cost per kWh (Y_o) is calculated as (17).

2) Pricing Interval Combination Without Charge Cycle Management: There is not charge cycle management as a response to the price signal. Here, pricing intervals combination is $\xi_w[k] = 1$ for $0 \leq k \leq T_N$ and $\xi_w[k] = 1$ for $T_N \leq k < T_{\text{in}}$, for this combination cost per kWh (Y_w) is calculated as (17).

3) Scheduled Pricing Interval Combination: Scheduled pricing intervals combination $\xi_s[k]$ for $0 \leq k < T_{\text{in}}$ is executed without adjustment on execution time, cost per kWh (Y_s) is calculated as (17).

4) Scheduled Pricing Interval Combination With Adjustment: Scheduled pricing intervals combination with adjustment on execution time $\xi_a[k]$ for $0 \leq k < T_{\text{in}}$ is executed, cost per kWh (Y_a) is calculated as (17).

B. Output Variables

Output variables from simulation scenario are the cost per kWh for each case (Y_o, Y_w, Y_s, and Y_a). To evaluate algorithm performance and advantage due to adjustment, percentage saving with respect to Y_w is calculated for the other three cases as

$$P_s = 100(Y_w - Y)/|Y_w| \tag{22}$$

where Y could be Y_o, Y_s, or Y_a depending on considered case.

Additionally, the algorithm is evaluated by comparing percentage saving owing to the algorithm (with and without adjustment) with the optimal percentage saving to know how close percentage saving due to the CCMA can get to the optimal percentage saving.

There are two additional output variables from the simulation scenario, they are the SoC obtained at the end of the charge cycle when the CCMA with and without adjustment is used. Because of adjusting the scheduled combination could imply that the charging process does not reach the desired final SoC, the impact on the final SoC must be evaluated. Percentage SoC error concerning SoC obtained when no adjustments are made is calculated as

$$e_{\text{SoC}} = 100\big(\text{SoC}_{fs} - \text{SoC}_{fa}\big)/\text{SoC}_{fs} \tag{23}$$

where SoC_{fs} is the final SoC due to executing scheduled combination and SoC_{fa} is the final SoC obtained because of adjusting scheduled combination on execution time.

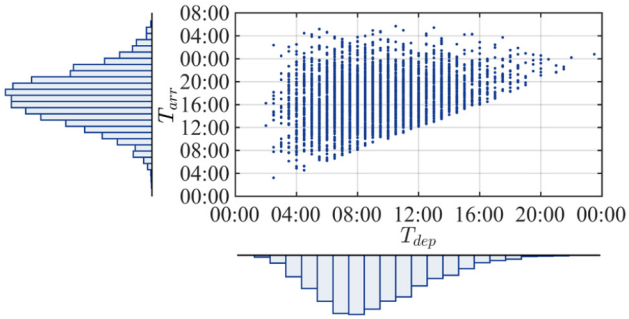

Fig. 10. Distribution of random samples (T_{arr}, T_{dep}) for simulation study.

C. Stochastic Models for Input Variables

SoC_i and the couple of time data (T_{arr}, T_{dep}) depend on EV user behavior and they must be stochastically modeled. The SoC_i depends on EV user driving behavior and the couple of time data (T_{arr}, T_{dep}) depend on EV user daily routine.

1) EV User Driving Behavior Model: Four cases are considered, for each one 3100 samples with different SoC_i distributions are generated.

1) *$SoC_i \sim N(\mu, \sigma^2)$:* With parameters $\mu = 0.5$ and $s = 0.1$, samples with probability distribution $P(\text{SoC}_i) = (1/(2ps^2)^{1/2})\exp(-(\text{SoC}_i - \mu)^2/2s^2)$.
2) *$SoC_i \sim U_{[a,b]}$:* With $a = 0.2$ and $b = 0.8$, SoC_i, samples with probability distribution $P(\text{SoC}_i) = 1/(b - a)$ if $a < \text{SoC}_i < b$, else $P(\text{SoC}_i) = 0$.
3) *$SoC_i \sim \text{Exp}(\lambda)$:* With parameter $\lambda = \mu^{-1} = 2$, samples with probability distribution $P(\text{SoC}_i) = \lambda\exp(-\lambda\text{SoC}_i)$.
4) *$SoC_i \sim Rician(v, \sigma)$:* With noncentrality parameter $v = 0$ and scale parameter $s = 0.3$, samples with probability distribution as (24), where $I_0(\cdot)$ is the first kind and zero order modified Bessel function

$$P(\text{SoC}_i) = \frac{\text{SoC}_i}{s^2}\left(e^{-\frac{\text{SoC}_i^2+s^2}{2s^2}}\right)I_0\left(\frac{v\text{SoC}_i}{s^2}\right). \tag{24}$$

2) EV User Daily Routine Model: The stochastic model proposed in [25] is used. T_{arr} distribution depends on T_{dep} distribution and can be expressed as a conditional probability distribution function (PDF). T_{arr} distribution is gotten adding T_{arr} distributions for each departure normalized time window $T_{\text{dep},i}$, that is: $P(T_{\text{arr}}) = \sum_{i=1}^{N} P(T_{\text{arr}}|T_{\text{dep},i})f(T_{\text{dep},i})$, where $f(T_{\text{dep},i})$ is the probability mass function of the ith departure time window $T_{\text{dep},i}$, N is the discrete number of $T_{\text{dep},i}$, and $P(T_{\text{arr}}|T_{\text{dep},i})$ is the conditional PDF of T_{arr} at $T_{\text{dep},i}$. The departure time probability mass function is modeled as a chi squared (χ^2) distribution $f(T_{\text{dep},i}) = ({T_{\text{dep},i}}^{(v-2)/2}e^{-T_{\text{dep},i}/2})/(2^{v/2}G(v/2))$, where the Gamma function $\Gamma(.)$ is defined as $\Gamma(z) = \int_0^{\chi}(t^{z-1}/e)\text{dt}$. $P(T_{\text{arr}}|T_{\text{dep},i})$ is adjusted as a Gaussian distribution for each $T_{\text{dep},i}$: $P(T_{\text{arr}}|T_{\text{dep},i}) = (2\pi\sigma_i^2)^{-1/2}\exp(-(T_{\text{arr}} - \mu_i)^2/(2\sigma_i^2))$, where μ_i and s_i are the mean and standard deviation of the ith departure time window. For each of the experiments, it is assumed that (T_{arr}, T_{dep}) reflect the next day (T_{arr}, T_{dep}). 3100 (T_{arr}, T_{dep}) samples are generated for simulation scenario as it is shown in Fig. 10.

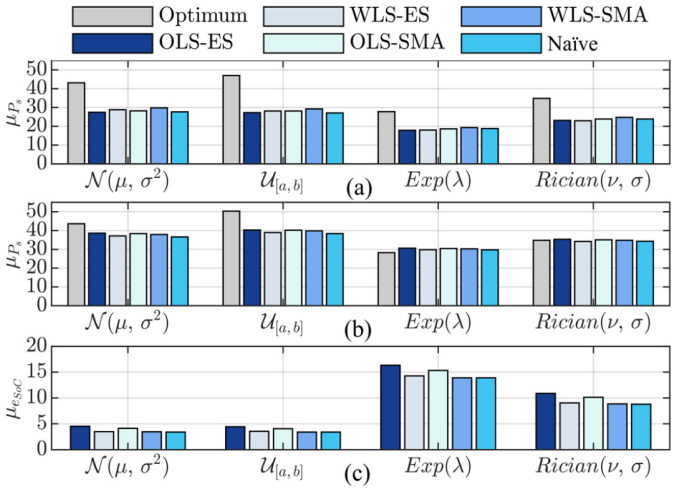

Fig. 11. Simulation results for each SoC_i distribution. (a) Mean of percentage saving without adjustment. (b) Mean of percentage saving with adjustment. (c) Mean of SoC error due to adjustment on execution time.

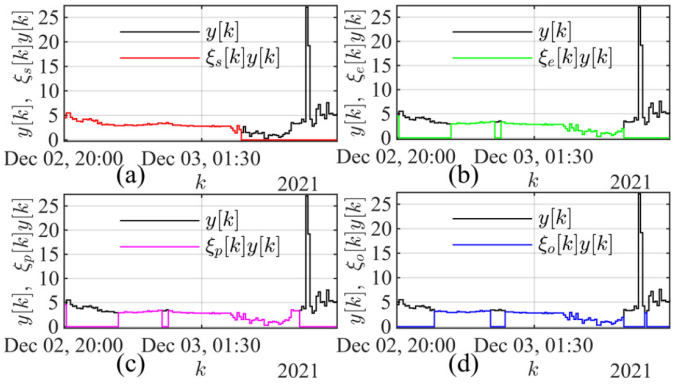

Fig. 12. Practical experiment 1 ($\text{SoC}_i = 25\%$) with OLS-ES: (a) without CCMA, (b) optimum, (c) scheduled combination, and (d) combination with adjustment.

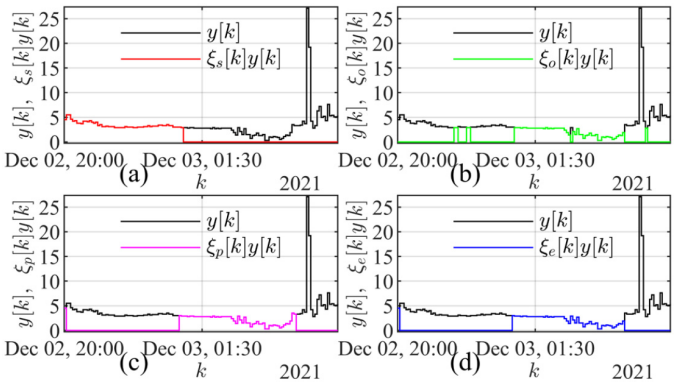

Fig. 13. Practical experiment 2 ($\text{SoC}_i = 50\%$) with OLS-ES: (a) without CCMA, (b) optimum, (c) scheduled combination, and (d) combination with adjustment.

D. Simulation Results

To evaluate algorithm performance (with and without adjustment), the means of percentage savings for all proposed price signal models are compared, a summary of simulation results is shown in Fig. 11. Percentage saving depends on user driving behavior, it is greater when SoC_i is normally or uniformly distributed. As it is shown in Fig. 11(a), when charge cycle management is performed according to scheduled combination, the means of percentage saving for all price signal models are considerable but less than the optimum. The greatest percentage saving is obtained when price signal forecasting is made with the WLS-SMA model for each considered driving behavior.

Alternatively, as it is shown in Fig. 11(b), when charge cycle management is performed with adjustments to scheduled combination on execution time, the means of obtained percentage saving for all price signal models is closer to the optimum and even greater than the optimum when driving behavior is exponentially or Rician distributed. The greatest percentage saving is obtained when price signal forecasting is made with the OLS-ES model for each considered driving behavior.

Even though adjustment on execution time could result in a percentage saving greater than the optimal one, it can have an impact on the final SoC reached at the end of the charging process. This impact is evidenced by the percentage SoC error (e_{SoC}) calculated as (23). As it is shown in Fig. 11(c), mean of e_{SoC} is greater when the user is likely to start the charging process with low SoC, that is, Exponentially or Rician distributed driving behavior. Therefore, the convenience of adjustment on execution time, as it was proposed, depends on user behavior and preference.

VII. Experimental Validation

To illustrate CCMS operation, three practical experiments are simultaneously conducted for the same day (Thursday, 2 December 2021), each one representing a different user driving behavior. The experiments consist in managing automatically in real time an EV charge cycle as a function of ComEd electricity price with different values for initial state of charge ($\text{SoC}_i = 25\%, 50\%,$ and 75%). The parameters for these simultaneously are $C = 80$ kWh, $\eta = 0.85$, $P_N = 10$ kW, $T_{\text{arr}} = 2021-12-02$ 20:00:00, $T_{\text{dep}} = 2021-12-03$ 07:00:00, and $\text{SoC}_f = 100\%$. Hence, $T_{\text{in}} = 132$ and $T_N = 85,\ 57,$ and 29.

As it is shown in Figs. 12–14, for each experiment, the four cases considered in the simulation scenario are considered: 1) optimal pricing intervals combination; 2) pricing interval combination without charge cycle management; 3) scheduled pricing interval combination; and 4) scheduled pricing interval combination with adjustment on execution time. The results of these experiments are shown in Table II, which is illustrated for each experiment and each case: the number of price intervals, the effect on SoC_f reached at the end of charging process, and the cost per kWh.

From all experiments can be concluded that there is a reduction in the cost of the charging cycle process when the CCMS is involved, which depends on SoC_i, being greater when user tend to arrive home with a greater SoC_i. Such that cost per kWh is nearly the same obtained with the optimal price intervals combination, especially when an adjustment

TABLE II
RESULTS FOR PRACTICAL EXPERIMENTS

Experiment	Fig.	T_N	SoC_f[%]	e_{SoC}[%]	Y[¢/kWh]	P_s[%]
$SoC_i = 25\%$	12(a)	85	100.3	-0.3	3.1918	0
	12(b)	85	100.3	-0.3	2.4024	24.73
	12(c)	85	100.3	-0.3	2.4494	23.26
	12(d)	81	96.7	3.3	2.4049	24.65
$SoC_i = 50\%$	13(a)	57	100.5	-0.5	3.4386	0
	13(b)	57	100.5	-0.5	2.0807	39.49
	13(c)	57	100.5	-0.5	2.1298	38.06
	13(d)	55	98.7	1.3	2.0836	39.41
$SoC_i = 75\%$	14(a)	29	100.7	-0.7	3.7414	0
	14(b)	29	100.7	-0.7	1.3586	63.69
	14(c)	29	100.7	-0.7	1.5138	59.54
	14(d)	29	100.7	-0.7	1.5172	59.44

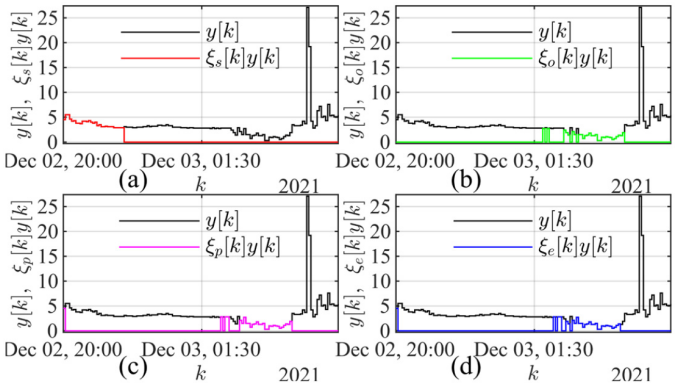

Fig. 14. Practical experiment 3 ($SoC_i = 75\%$) with OLS-ES: (a) without CCMA, (b) optimum, (c) scheduled combination, and (d) combination with adjustment.

is realized during execution. However, adjustments in execution time could affect the SoC_f reached at the end of the charging process because the charging process is performed within fewer price intervals. Such effect depends on SoC_i, being greater when user tends to arrive home with a smaller SoC_i. On the other hand, the CCMS performs the charging process in lower price intervals, avoiding price intervals with higher prices when energy demand is greater.

VIII. CONCLUSION AND FUTURE WORK

The proposed CCMS was conceived as a DSM IoT solution for a smart charger with a simple network architecture that only requires a residential AP to access the Internet. In contrast, to centralize DSM IoT solutions [14]–[17], with more complex network architectures, the proposed CCMS does not affect EV user privacy because it does not require sharing user consumption behavior data.

It was experimentally validated that the proposed CCMS can automatically manage EVs charge cycle in real time as a function of the ComEd RTP signal. Additionally, the proposed CCMA was evaluated through a simulation study. It was found that the proposed CCMS is a suitable DMS solution to reduce consumption at high demand intervals since EV charge cycles are performed at the lowest price interval combinations. Thus, the EV user gets a reduction in the total cost of the EV charge cycle and the EV user consumption is reduced when grid operation requires it. In the simulation, it was also evaluated the effect of user driving behavior on such percentage saving when the proposed CCMA is implemented as a DSM strategy in the ComEd RTP scheme.

Since the battery life cycle is a critical factor that determines EVs cost and affects its autonomy, battery depletion due to pulsating and discontinuous charge cycle must be considered. Currently, we are working on estimating the impact of the proposed CCMS on battery depletion to improve the proposed CCMA. Considering such impact as well as ComEd RTP signal when scheduling charge cycle could help to determine and enhance the real economic benefit owing to the CCMS implementation.

REFERENCES

[1] A. Masoum, S. Deilami, P. Moses, M. Masoum, and A. Abu-Siada, "Smart load management of plug-in electric vehicles in distribution and residential networks with charging stations for peak shaving and loss minimization considering voltage regulation," *IET Gener. Transm. Distrib.*, vol. 5, no. 8, pp. 877–878, Aug. 2011, doi: 10.1049/iet-gtd.2010.0574.

[2] H. Mortaji, S. H. Ow, M. Moghavvemi, and H. A. F. Almurib, "Load shedding and smart-direct load control using Internet of Things in smart grid demand response management," *IEEE Trans. Ind. Appl.*, vol. 53, no. 6, pp. 5155–5163, Nov./Dec. 2017, doi: 10.1109/TIA.2017.2740832.

[3] R. Tang, S. Wang, and C. Yan, "A direct load control strategy of centralized air-conditioning systems for building fast demand response to urgent requests of smart grids," *Autom. Construct.*, vol. 87, pp. 74–83, Mar. 2018, doi: 10.1016/j.autcon.2017.12.012.

[4] A. Taşcıkaraoğlu, N. G. Paterakis, O. Erdinç, and J. P. S. Catalão, "Combining the flexibility from shared energy storage systems and DLC-based demand response of hvac units for distribution system operation enhancement," *IEEE Trans. Sustain. Energy*, vol. 10, no. 1, pp. 137–148, Jan. 2019, doi: 10.1109/TSTE.2018.2828337.

[5] F. L. Müller and B. Jansen, "Large-scale demonstration of precise demand response provided by residential heat pumps," *Appl. Energy*, vol. 239, pp. 836–845, Apr. 2019, doi: 10.1016/j.apenergy.2019.01.202.

[6] F. Varasteh, M. Nazar, A. Heidari, M. Shafie-khah, and J. Catalão, "Distributed energy resource and network expansion planning of a CCHP based active microgrid considering demand response programs," *Energy*, vol. 172, pp. 79–105, Apr. 2019, doi: 10.1016/j.energy.2019.01.015.

[7] A. Bostan, M. Nazar, M. Shafie-khah, and J. P. S. Catalão, "Optimal scheduling of distribution systems considering multiple downward energy hubs and demand response programs," *Energy*, vol. 190, Jan. 2020, Art. no. 116349, doi: 10.1016/j.energy.2019.116349.

[8] K. Stenner, E. Frederiks, E. Hobman, and S. Cook, "Willingness to participate in direct load control: The role of consumer distrust," *Appl. Energy*, vol. 189, pp. 76–88, Mar. 2017, doi: 10.1016/j.apenergy.2016.10.099.

[9] C. Chen, J. Wang, and S. Kishore, "A distributed direct load control approach for large-scale residential demand response," *IEEE Trans. Power Syst.*, vol. 29, no. 5, pp. 2219–2228, Sep. 2014, doi: 10.1109/TPWRS.2014.2307474.

[10] J. Touma *et al.*, "Energy management system of microgrid: Control schemes, pricing techniques, and future horizons," *Int. J. Energy Res.*, vol. 45, no. 9, pp. 12728–12739, Jul. 2021, doi: 10.1002/er.6714.

[11] M. Sulaima, N. Dahlan, Z. Yasin, M. Rosli, Z. Omar, and M. Hassan, "A review of electricity pricing in peninsular Malaysia: Empirical investigation about the appropriateness of enhanced Time of use (ETOU)electricity tariff," *Renew. Sustain. Energy Rev.*, vol. 110, pp. 348–367, Aug. 2019, doi: 10.1016/j.rser.2019.04.075.

[12] D. Jay and K. S. Swarup, "A comprehensive survey on reactive power ancillary service markets," *Renew. Sustain. Energy Rev.*, vol. 144, Jul. 2021, Art. no. 110967, doi: 10.1016/j.rser.2021.110967.

[13] A. Amin *et al.*, "A review of optimal charging strategy for electric vehicles under dynamic pricing schemes in the distribution charging network," *Sustainability*, vol. 12, no. 23, pp. 1–28, Dec. 2020, doi: 10.3390/su122310160.

[14] Y. Wang, S. Mao, and R. M. Nelms, "Distributed online algorithm for optimal real-time energy distribution in the smart grid," *IEEE Internet Things J.*, vol. 1, no. 1, pp. 70–80, Feb. 2014, doi: 10.1109/JIOT.2014.2305667.

[15] R. Jackson, S. Sankaranarayanan, and J. Rodrigues, "Smart energy management and demand reduction by consumers and utilities in an IoT-fog based power distribution system," *IEEE Internet Things J.*, vol. 6, pp. 7386–7394, Oct. 2019, doi: 10.1109/JIOT.2019.2894326.

[16] V. Caballero, D. Vernet, and A. Zaballos, "Social Internet of Energy—A new paradigm for demand side management," *IEEE Internet Things J.*, vol. 6, pp. 9853–9867, Dec. 2019, doi: 10.1109/JIOT.2019.2932508.

[17] A. Kumar, F. Mahfoudhi, and J. Famaey, "Real-time demand respond using NB-IoT," *IEEE Internet Things J.*, vol. 7, pp. 11863–11872, Dec. 2020, doi: 10.1109/JIOT.2020.3004390.

[18] S. Tanwar, S. Tyagi, and S. Kumar, "The Role of Internet of Things and smart grid for the development of a smart city," in *Intelligent Communication and Computational Technologies* (Lecture Notes in Networks and Systems), vol. 19. Singapore: Springer, Oct. 2017, pp. 23–33, doi: 10.1007/978-981-10-5523-2_3.

[19] R. Babu, V. Amudha, C. Chellaswamy, and K. Senthil, "IoT based residential energy management system for demand side response through load transfer with various types of domestic appliances," *Build. Simulat.*, vol. 15, p. 1703, Aug. 2021, doi: 10.1007/s12273-021-0817-4.

[20] S. Hashmi, C. Ali, and S. Zafar, "Internet of Things and cloud computing-based energy management system for demand side management in smart grid," *Int. J. Energy Res.*, vol. 45, pp. 1007–1022, Jan. 2021, doi: 10.1002/er.6141.

[21] S. Ali and B. Choi "State-of-the-art artificial intelligence techniques for distributed smart grids: A review," *Electronics*, vol. 9, no. 6, pp. 1–28, Jun. 2020, doi: 10.3390/electronics9061030.

[22] A. Miglani, N. Kumar, V. Chamola, and S. Zeadally, "Blockchain for Internet of Energy management: Review, solutions, and challenges," *Comput. Commun.*, vol. 151, pp. 395–418, Feb. 2020, doi: 10.1016/j.comcom.2020.01.014.

[23] G. Dileep, "A survey on smart grid technologies and applications," *Renew. Energy*, vol. 146, pp. 2589–2625, Feb. 2020, doi: 10.1016/j.renene.2019.08.092.

[24] (Commonwealth Edison Company, Chicago, IL, USA). *ComEd Hourly Price API*. Accessed: Nov. 2, 2021. [Online]. Available: https://hourlypricing.comed.com/hp-api/

[25] T. Lee, Z. Bareket, T. Gordon, and Z. S. Filipi, "Stochastic modeling for studies of real-world PHEV usage: Driving schedule and daily temporal distributions," *IEEE Trans. Veh. Technol.*, vol. 61, no. 4, pp. 1493–1502, May 2012, doi: 10.1109/TVT.2011.2181191.

[26] W. Min and S. Weinan, "Analysis on 2-element insertion sort algorithm," in *Proc. Int. Conf. Comput. Design Appl. (ICCDA)*, vol. 1, pp. V1-143–V1-146, Jun. 2010, doi: 10.1109/ICCDA.2010.5541165.

Miguel Ángel Dávila Rojas received the B.S. degree in electronics engineering and the M.Sc. degree in information and communications from the Universidad Distrital Francisco José de Caldas, Bogotá, Colombia, in 2015 and 2021, respectively.

His main research interests include modeling and state estimation of electric batteries, development of energy conversion systems for electric vehicles charging applications, and development of energy management systems.

César Leonardo Trujillo Rodríguez received the B.S. degree in electronics engineering from the Universidad Distrital Francisco José de Caldas, Bogotá, Colombia, in 2003, the M.Sc. degree in electrical engineering from the Universidad Nacional de Colombia, Bogotá, in 2006, and the Ph.D. degree in electronics engineering from the Universidad Politécnica de Valencia, Valencia, Spain, in 2012.

He is a Full Professor with the Department of Electrical Engineering, Universidad Distrital Francisco José de Caldas, where he currently teaches courses on analog circuits and power electronics. His main research interests include modeling and control of power converters applied to the distributed generation and microgrids.